Acta Oceanol. Sin., 2012, Vol. 31, No. 5, P. 98-106
DOI: 10.1007/s13131-012-0240-x
http://www.hyxb.org.cn
E-mail: hyxbe@263.net

Spatial and temporal variability of colored dissolved organic matter absorption properties in the Taiwan Strait

LIN Hui[1,2], GUO Weidong[1*], HU Minghui[1], LIN Cai[2], JI Weidong[2]

[1] College of Ocean and Earth Sciences, Xiamen University, Xiamen 361005, China

[2] Third Institute of Oceanography, State Oceanic Administration, Xiamen 361005, China

Received 30 April 2011; accepted 3 August 2011

Abstract
Spatial and temporal variability of the absorption properties of colored dissolved organic matter (CDOM) in the Taiwan Strait was investigated in summer (July to August of 2006) and winter (from December 2006 to January of 2007) seasons. The CDOM absorption coefficient at 280 nm (a_{280}) showed a decreasing trend from nearshore to offshore areas while the spectral slope coefficient parameter calculated between wavelengths 275–295 nm ($S_{275-295}$) showed an increase, indicative of decreasing aromaticity and molecular weight of the CDOM. The average a_{280} in winter (1.47±0.50 m^{-1}) was significantly higher than in summer (1.10±0.41 m^{-1}), while the average $S_{275-295}$ in winter (26.7±5.2 μm^{-1}) was significantly lower than in summer (30.6±5.5 μm^{-1}), demonstrating clear seasonal variation in CDOM abundance and properties in the Taiwan Strait. A three-end-member conservative mixing model showed that local terrestrial CDOM inputs from several rivers along the western coast were small (<5%). However, the distribution of CDOM in the Taiwan Strait is mainly controlled by water mass movement [i.e., the Zhe-min Coastal Current (ZCC) and the Kuroshio Branch Current (KBC) in winter and the South China Sea Water (SCSW) in summer]. Biological activity was also an important factor affecting the distribution of CDOM in the offshore region in summer months.

Key words: colored dissolved organic matter, absorption properties, seasonal variation, hydrology, Taiwan Strait

1 Introduction

Colored dissolved organic matter (CDOM) is the component of dissolved organic matter that absorbs light in the ultraviolet and visible ranges of the electromagnetic spectrum (Bricaud et al., 1981; Guo et al., 2007; Helms et al., 2008; Yamashita et al., 2010). As the optically active fraction of dissolved organic matter (DOM), CDOM has a strong impact on the availability and spectral quality of light in marine regions (Blough and Del Vecchio, 2002), thus affecting processes like primary production. CDOM light absorption is the highest in the ultraviolet region and declines to near-zero levels in the red region of the spectrum, making it a key parameter with respect to satellite retrieval of phytoplankton pigments and suspended particulate material (Doxaran et al., 2002; Stedmon et al., 2010). Furthermore, the absorption spectral parameters of CDOM can also provide quantitative and qualitative information on DOM (Stedmon et al., 2000; Helms et al., 2008; Guo et al., 2007, 2010).

The distribution and optical properties of CDOM in coastal waters are influenced by many physical, chemical and biological processes, such as the dilution of terrestrially-derived CDOM, photochemical bleaching, bacterial degradation and autochthonous production of CDOM by plankton (Kowalczuk et al., 2009). Terrestrial CDOM may be a conservative or quasi-conservative constituent of water when allochthonous supply and mixing rates exceed autochthonous production and degradation (Guo et al., 2007; Stedmon et al., 2010). In such cases, optical properties of water masses (such as CDOM absorption) can be utilized to

Foundation item: Scientific Research Foundation of Third Institute of Oceanography, State Oceanic Administration under contract No. TIO 2009007; the National Natural Science Foundation of China under contract No. 41276064; Fujian Provincial Surveys of Marine Chemistry in Coastal Waters and Harbours under contract No. FJ908-04-07; River Basin-Estuary Ecological Security Assessment and Management Strategy under contract No. 200805064; the National 908 Surveys of Marine Chemistry in Coastal Waters under contract No. 908-ZC-I-03; the Fujian Provincial 908 Project under contract No. FJ-01-01-HS(chemistry).
*Corresponding author, E-mail: wdguo@xmu.edu.cn

trace the mixing of water masses (Stedmon and Markager, 2003; Granskog et al., 2007; Jiang et al., 2008). Due to the highly variable and complex nature of hydrology in different coastal waters in the world, the influence of hydrology (i.e., river discharge) on CDOM sources, spatial and temporal variations should be tested in more coastal waters, of which the Taiwan Strait provides an ideal study site.

The Taiwan Strait, bounded by China Mainland to the west and the island of Taiwan to the east, is a narrow passage that connects the East China Sea with the South China Sea. Its width, length and average depth is about 180 km, 350 km and 60 m respectively (Jan et al., 2002; Lan et al., 2009). In this region, a strong seasonal variation in oceanographic conditions is associated with both the dry winter northeasterly monsoon (November–February) and the wet summer southwesterly monsoon (May–August) (Kester et al., 1993). The Minjiang River and Jiulongjiang River provide allochthonous terrestrial CDOM sources to the Taiwan Strait (Guo et al., 2007; Du et al., 2010, Guo et al., 2011a, b). However, the optical properties of CDOM for the whole strait are rarely reported. In addition, the relationship between the distribution of CDOM and water mass movements in the Taiwan Strait needs to be expatiated. The multi-end-member mixing model representing the different allochthonous CDOM sources suitable for other coastal waters (Stedmon et al., 2010) needs to be tested in this channel sea area with its complex hydrodynamic environment (Hu et al., 2010). Based on data collected during summer and winter seasons, spatial and temporal variability of absorption properties of CDOM in the Taiwan Strait was investigated. The influence of hydrology on the distribution of CDOM is also discussed.

2 Materials and methods

2.1 *Sample collection*

Field surveys were carried out during two cruises from July to August of 2006 (summer) and from December 2006 to January of 2007 (winter) (Fig. 1). Water samples were taken using 5-L Niskin bottles attached to a standard conductivity-temperature-depth (CTD) rosette. Two to four depths were sampled depending on the total water depth of the sampling station. One hundred and ten samples from 38 stations and 110 samples from 35 stations were collected for summer and winter cruises, respectively. After collection, all samples were immediately filtered through 0.2 μm Millipore polycarbonate membrane filters. The filtrates were stored at 4℃ and in the dark until analysis

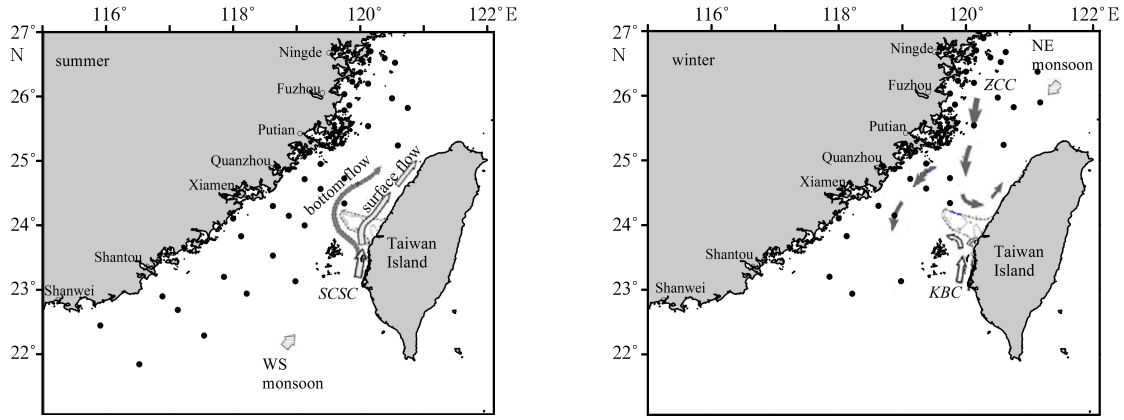

Fig.1. Location of the sampling stations in the Taiwan Strait. The arrows indicating the main currents in the Taiwan Strait in summer (left) and winter (right), cited from Jan et al. (2002).

in the laboratory within two weeks after each cruise.

2.2 *CDOM absorption measurements*

The absorbance of CDOM was scanned in the range from 240 to 800 nm using a 10 cm quartz cuvette with Techcomp UV-2300 spectrophotometer. Milli-Q water was used as a reference. The absorption coefficient was calculated from optical density (A) according to Eq. (1) and Eq. (2):

$$a_{(\lambda)} = 2.303A_{(\lambda)}/L, \tag{1}$$

where L is the length of the cuvette (m).

The CDOM absorption spectra can then be modeled with Eq. (2):

$$a_{(\lambda)} = a_{(\lambda_0)}e^{-S_{(\lambda_0-\lambda)}} + k, \tag{2}$$

where $a_{(\lambda)}$ is the absorption coefficient at a wavelength λ and λ_0 is a reference wavelength, S is the spectral slope and k is the background parameters used to correct for scattering or baseline shift in longer wavelength region of absorption spectra (Stedmon et al., 2000; Guo et al., 2007).

In this study, the absorption coefficient of CDOM at 280 nm (a_{280}) was used as an estimate for CDOM concentration. The spectral slope (S) parameter between 275–295 nm was calculated by Eq. (2) using a non-linear regression technique with Matlab software. This $S_{275-295}$ value was suggested to be a good proxy for DOM molecular weight (Helms et al., 2008), with much lower $S_{275-295}$ for terrestrial DOM in comparison with the marine endmember in an estuarine and coastal environment.

2.2 *Statistical analyses*

SPSS 11.0 software (Statistical Program for Social Sciences) was used for statistical analysis in this study. Differences in the absorption features of CDOM between the two seasons, such as the absorption coefficient (a_{280}) and the spectral slope ($S_{275-295}$) were assessed with an independent sample t-test, using a p value of 0.05 to determine the significance. Correlation analysis and principle component analysis (PCA) were used to examine the relationships between variables and to estimate the contribution of biological activity and water mass mixing to the distribution of CDOM in the Taiwan Strait, respectively.

3 Results

3.1 *General hydrography of the Taiwan Strait*

3.1.1 *Summer hydrography*

Winds over the Taiwan Strait are dominated by the East Asia monsoon, from northeast in winter to southwest in summer. With the aid of summer stratification and southwest monsoon, the northward intrusion of SCSW (the South China Sea Water) surface flow in summer is relatively unimpeded. The relatively cold SCSW bottom flow, blocked by the Changyun Rise (CYR), distributed in the west of the Straits around CYR (Jan et al., 2002). The South China Sea and the Kuroshio waters, entering into the Taiwan Strait from the Southern Strait, have similar high temperature and high salinity properties. The coastal water formed when the SCSW surface flow mixes with continental runoff (Xiao and Cai, 1988).

The T-S diagram of the Taiwan Strait in summer cruise of 2006 corroborated the above analysis (Fig. 2a). These data indicate that three endmembers exist when water masses with different properties are mixed. These endmembers include Continental runoff (high temperature and low salinity)the SCSW surface flow (high temperature and high salinity) and the SCSW bottom flow (low temperature and high salinity), respectively.

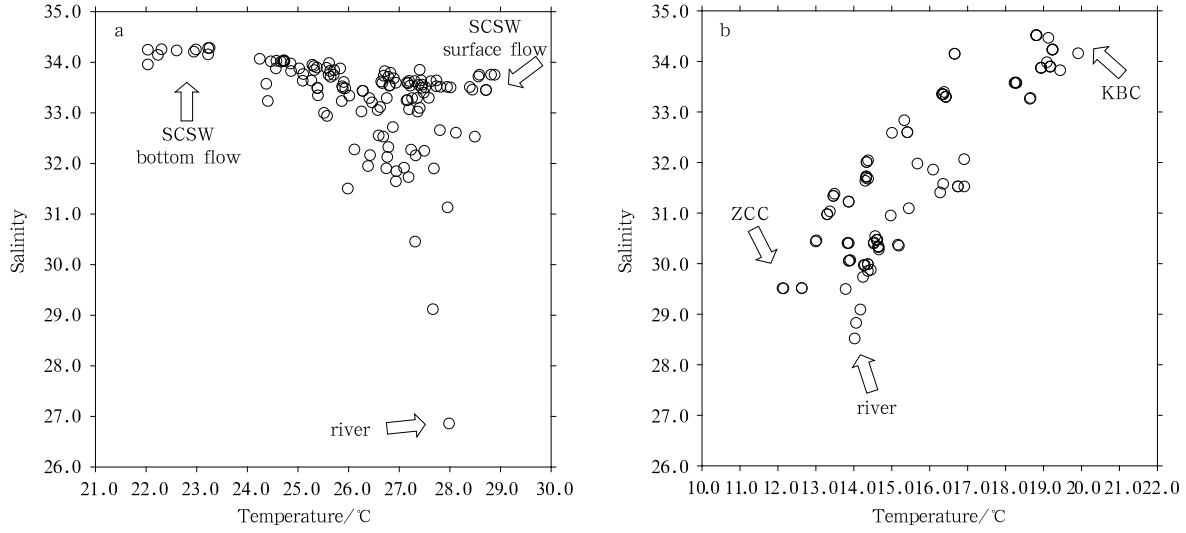

Fig.2. T-S diagram of the Taiwan Strait during summer (a) and winter (b) cruises.

3.1.2 *Winter hydrography*

The Zhe-min Coastal Current (ZCC), mainly formed from a mixture of continental runoff and coastal seawater, is the major water mass in the Taiwan Strait during winter. It may reach the vicinity of the Dongshan Island (Wu, 1982) or even penetrate as

far south as the Nan'ao Island (Xiao and Cai, 1988). A portion of this coastal current is deflected by CYR and turns back northeastward. The T-S diagram of the Taiwan Strait in winter is shown in Fig. 2b. It is clear that three water masses exist in this season. Besides the Zhe-min Coastal Current (ZCC), the Kuroshio Branch Current (KBC) and the continental runoff input also exist (Fig. 2b).

3.2 *Distributions of CDOM optical properties*

The absorption coefficient (a_{280}) and spectral slope ($S_{275-295}$) of CDOM in two seasons were shown in Table 1. In summer, the ranges of a_{280} and $S_{275-295}$ for whole salinity gradient (26.855 1–34.278 2) were 0.54–2.48 m^{-1} and 20.0–45.3 μm^{-1}. In winter, the ranges of a_{280} and $S_{275-295}$ for whole salinity gradient (28.514 3–34.512 7) were 0.55–2.83 m^{-1} and 19.6–44.6 μm^{-1}. The average a_{280} (1.47±0.50 m^{-1}) in winter was significantly higher than that (1.10±0.41 m^{-1}) in summer (t-test, p <0.001) and the average $S_{275-295}$ (26.7±5.2 μm^{-1}) in winter was significantly lower than that (30.6±5.5 m^{-1}) in summer (t-test, p <0.001), suggesting that there was a greater terrestrial CDOM signal during the winter season in the Taiwan Strait, as CDOM from terrestrial sources usually has a higher absorption coefficient and lower spectral slope values than those from marine sources.

Figure 3 shows the horizontal distributions of a_{280} and $S_{275-295}$ in surface waters at different seasons. a_{280} was relatively high in the nearshore waters, but decreased to the offshore region. However, the observed trend in $S_{275-295}$ was the opposite, particularly pronounced in winter. This obviously reflects the contribution of terrestrial CDOM input in coastal waters. In summer, relatively high a_{280} (>2.0 m^{-1}) was located in the vicinity adjacent to the Jiulongjiang River Estuary, Xinhua Bay and Minjiang River Estuary. The values of $S_{275-295}$ in most nearshore areas were less than 25 μm^{-1}. In winter, the area of relatively high a_{280} (>2.0 m^{-1}) was much larger, covering the near shore region from the Quanzhou Bay to the north of the Minjiang River Estuary, but the input from the Jiulongjiang River Estuary decreased. The spectral slope showed a clear gradient, with lower values (<25 μm^{-1}) in the coastal zone and highest values (>40 μm^{-1}) in the east of the central Taiwan Strait.

Table 1. Absorption coefficient (a_{280}) and spectral slope ($S_{275-295}$) values in the Taiwan Strait

Cruises	Layer	Range of salinity	Mean of salinity	a_{280}/m^{-1}	Mean of a_{280}/m^{-1}	Range of $S_{275-295}/\mu m^{-1}$	Mean of $S_{275-295}/\mu m^{-1}$
Summer	surface	26.855 1–33.819 6	32.689 3	0.65–2.48	1.21	20.0–45.3	30.1
	10 m	31.896 2–33.840 4	33.285 0	0.67–2.25	1.12	22.6–44.8	31.3
	30 m	33.452 5–34.278 2	33.812 4	0.68–1.70	0.96	28.3–37.5	32.1
	bottom	31.498 6–34.276 7	33.696 8	0.54–2.11	1.03	21.7–44.6	29.9
	total	26.855 1–34.278 2	33.286 2	0.54–2.48	1.10	20.0–45.3	30.6
Winter	surface	28.514 3–34.512 7	31.859 2	0.55–2.62	1.53	19.6–44.6	26.5
	10 m	29.087 5–34.512 6	31.918 3	0.65–2.83	1.52	20.4–44.0	26.5
	30 m	29.969 5–34.425 3	32.946 1	0.72–2.44	1.22	19.8–37.0	28.1
	bottom	29.492 7–34.512 0	32.012 5	0.68–2.40	1.48	20.2–42.4	26.2
	total	28.514 3–34.512 7	32.072 9	0.55–2.83	1.47	19.6–44.6	26.7

The horizontal distributions of these optical properties in other water layers were similar to those of surface layer, suggesting that the main factors controlling the distribution of CDOM were similar in different layers, although some differences occurred in the abundance of a_{280} and $S_{275-295}$ (Table 1).

3.3 *Relationships between CDOM optical properties and salinity*

The relationships between a_{280} and $S_{275-295}$ with salinity are shown in Fig. 4. Overall, a_{280} decreased with the increase of salinity in both seasons. The values of $S_{275-295}$ changed little when the salinity was less than 32, but increased markedly at higher salinities. These results indicate a relatively strong mixing process controlling the distribution of CDOM in the Taiwan Strait, especially in winter. The scattering of data points implies that whether in winter or summer, there could be several endmembers for CDOM in this region, which will be discussed in detail later.

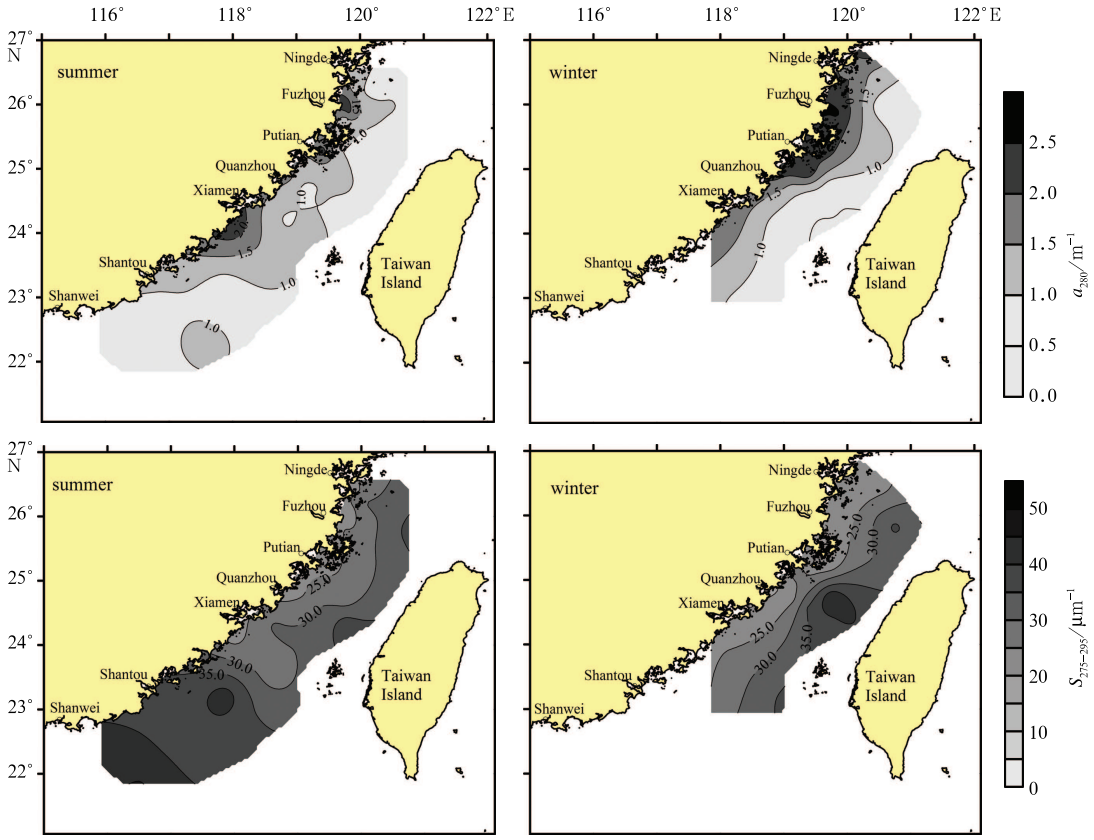

Fig.3. Horizontal distributions of a_{280} and $S_{275-295}$ in surface waters.

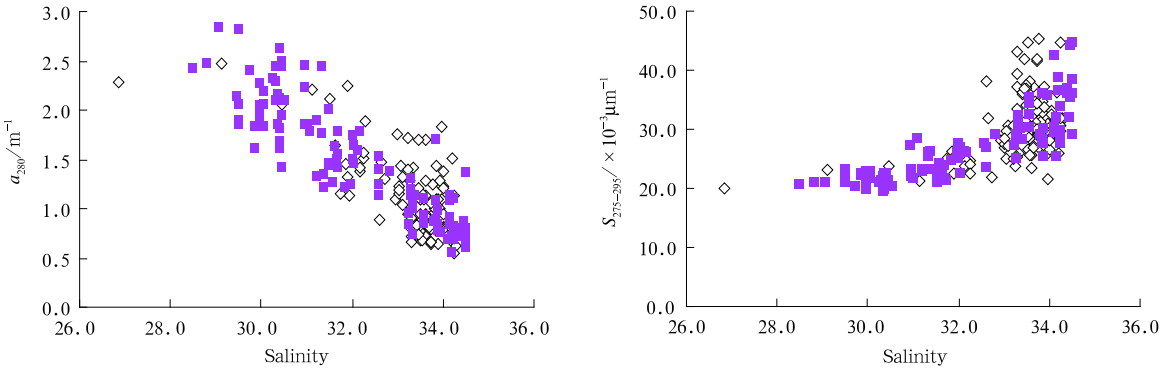

Fig.4. Absorption coefficient at 280 nm (a_{280}) and the spectral slope ($S_{275-295}$) versus salinity. The open squares represent summer samples while solid circles represent winter samples.

4 Discussion

4.1 *Hydrography influence on CDOM distribution*

As described in 3.1, the hydrography in the Taiwan Strait shows obvious seasonal variation. This will undoubtedly influence the distribution of CDOM in the region. In summer, the mixing process between the continental runoff and SCSW surface flow occurs in the upper layer of the nearshore waters. The horizontal variation of salinity in surface layer and the depth of the thermocline showed that this zone of mixing is in the range from the surface to 20 m depth and within the area with salinity not more than 32.5 (Fig. 5). The variation of spectral slope ($S_{275-295}$) in this salinity range was also small compared with the higher

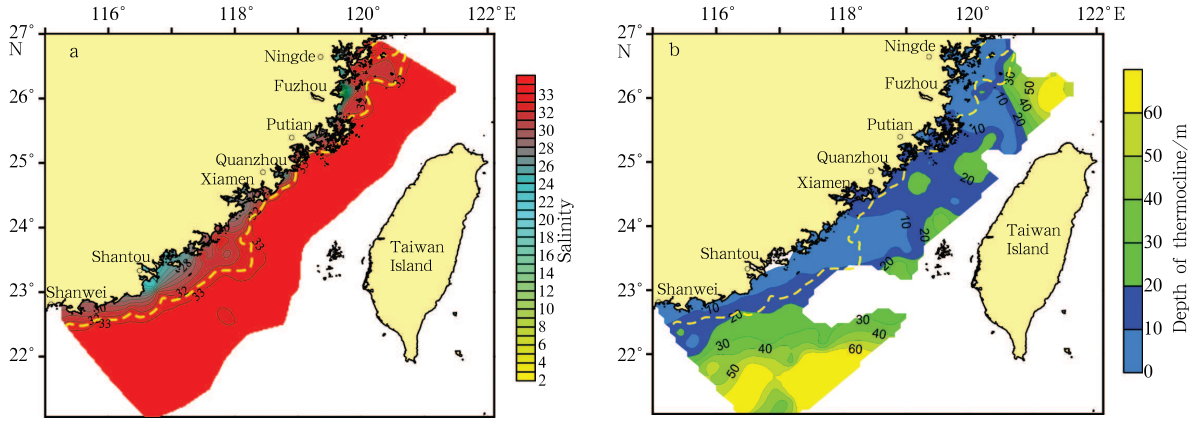

Fig.5. Horizontal distribution of salinity in surface layer (a) and the depth of the thermocline (b) in summer. The dotted lines represent the isoline of salinity at 32.5 in surface layer.

variation observed when salinity was greater than 32.5 (Fig. 2).

a_{280} generally tended to decrease with increasing salinity in an approximately linear fashion with salinity ranges of not more than 32.5 in summer (Table 2), indicating that a strong mixing occurred between CDOM derived from continental runoff and SCSW surface flow. On the contrary, no significant correlation is observed between a_{280} and salinity in higher salinity region (>32.5) (Table 2), suggesting that terrestrial inputs did not influence the CDOM distribution in offshore waters of the Taiwan Strait in this season. Instead, the dominant CDOM source in this offshore region was from SCSW surface flow and bottom flow, driven by the summer southwest monsoon.

Table 2. Relationships between a_{280} and salinity in different salinity region

Season	Salinity region	Parameter	Range	Mean	Correlation with salinity			
					n	A	B	r
Summer	⩽32.5	a_{280}	1.14–2.48	1.73	16	–0.200 1	7.983 4	0.652 2*
		$S_{275-295}$	20.1–26.2	23.6				
	>32.5	a_{280}	0.54–1.84	1.00	94	–0.219 8	8.387 9	0.285 8*
		$S_{275-295}$	21.7–45.3	31.7				
Winter	⩽32.0	a_{280}	1.21–2.82	1.94	57	–0.321 0	11.749 0	0.634 2*
		$S_{275-295}$	19.5–28.3	22.3				
	>32.0	a_{280}	0.69–1.73	1.07	53	–0.267 1	10.021 0	0.670 2*
		$S_{275-295}$	22.5–38.6	29.4				

Notes: The units for a_{280} and $S_{275-295}$ are m^{-1} and μm^{-1}, respectively. * p <0.01.

During the winter season, the water appears to be very well mixed in the whole water column and the phenomena of stratification disappeared. Furthermore, the Zhe-min Coastal Current (ZCC) characterized by low temperatures (<20℃) and low salinities (salinity⩽32.0) moved southward along the western boundary of the Taiwan Strait (Jan et al., 2002) from December in 2006 to February in 2007. In the influence area of the ZCC, a strong negative correlation was observed between a_{280} and salinity (Table 2), indicating a physical mixing between continental runoff and the ZCC. A strong linear regression was also observed for the high salinity region (>32.0) but with a much lower slope (Table 2), suggesting that water mass mixing also occurred in offshore waters of the Taiwan Strait in winter. This is contrary to the summer season. Based on the hydrography data, the CDOM endmembers were ZCC and KBC, respectively.

From the regression equations in Table 2, the apparent abundance of a_{280} for continental runoff can also be inferred. It was 7.96 m^{-1} in summer and 11.71 m^{-1} in winter if salinity of the terrestrial endmember is assumed to be 0.1. It should be emphasized that these values were the synthesized results for many local rivers along the west coast of the Strait. These inferred results are consistent with the limited data in

local rivers. For example, the average a_{280} in the main stream of the Minjiang River in summer is 8.87 m^{-1} (Guo et al., 2011a), while the average a_{280} of the Jiulongjiang River in summer and winter is 7.35 and 9.34 m^{-1}, respectively (Hong et al., 2012). It is easy to see that the CDOM abundance of the river endmembers in winter is higher than that in summer. This may be due to the dilution effect of river CDOM by water discharge during the summer wet season. In addition, the contributions of terrestrial CDOM input from the Minjiang River, the Jiulongjiang River and some rivers flowing into the Xinhua Bay showed large variation in different seasons (Fig. 3).

4.2 *Contribution of biological activity on CDOM distribution: Principal component analysis*

CDOM derives from allochthonous and autochthonous sources in aquatic ecosystems. Runoff is generally assumed to be the dominant allochthonous source of CDOM in coastal waters. For autochthonous CDOM, phytoplankton is one of the most important contributors (Rochelle-Newall and Fisher, 2002; Guo et al., 2011a; Hong et al., 2012). In certain eutrophic areas, phytoplankton degradation becomes the main controlling factor affecting the optical properties and nutrient cycling of aquatic environment (Zhang et al., 2009).

To evaluate the contribution of such biological activity to the CDOM load in the Taiwan Strait, a principal component analysis (PCA) including chlorophyll a, temperature, salinity and a_{280} was carried out. Temperature and salinity represent the characteristics of the water masses, while chlorophyll a and a_{280} are indicators of biological activities and abundance of CDOM. Thus, the relative importance of water masses mixing and phytoplankton primary production on CDOM distribution can also be revealed by this statistical approach. Whether in summer or in winter, four parameters (temperature, salinity, a_{280} and chlorophyll a) were translated into two primary components (Component 1 and Component 2) (Table 3), suggesting that the distribution of optical properties for CDOM in the Taiwan Strait could be revealed by two unrelated components according to the results of the PCA.

In the area with salinity lower than 32.5 in summer and all areas in winter, the primary Component 1 included temperature, salinity and a_{280} while the primary Component 2 only contained chlorophyll a. The percent of total variance explained for Component 1 and Component 2 ranged from 52.4% to 69.0% and from 24.2% to 31.7%, respectively, which implied that the concentration level and the distribution of CDOM were mainly affected by water masses mixing in the Taiwan Strait. In other words, the mixing of water masses with different character was the main controlling factor influencing the CDOM spatial distribution. While biological activity, especially photosynthesis and degradation of phytoplankton, played a minor role in affecting the CDOM distribution relative to water mass mixing. This is further supported by the insignificant correlation relationship between a_{280} and chlorophyll a.

Table 3. Results of PCA in the Taiwan Strait

Item	Summer				Winter			
	Salinity≤32.5		Salinity>32.5		Salinity≤32.0		Salinity>32.0	
Variables	1	2	1	2	1	2	1	2
Temperature	0.758	–0.294	0.745	–0.561	0.835	0.395	0.930	–0.153
Salinity	–0.879	–0.235	–0.918	0.098	0.792	–0.446	0.973	–0.023
Chl a	0.140	0.965	0.323	0.695	0.533	0.776	0.254	0.967
a_{280}	0.854	–0.139	0.436	0.651	–0.699	0.558	–0.939	0.085
Percentage of total variance explained	52.4	27.3	42.3	30.7	52.4	31.7	69.0	24.2
Possible controlling factor	WM	BA	WM	BA	WM	BA	WM	BA

Notes: WM representes water masses mixing, BA biological activity.

However, in the region with salinity higher than 32.5 in summer, the Component 1 only included temperature and salinity while the Component 2 contained both a_{280} and chlorophyll a. The percentage of total variance explained for Component 1 and Component 2 was 42.3% and 30.7%, respectively. In addition, there was a linear correlation between chlorophyll a and a_{280} (r =0.265, p <0.05). These results imply an increasing contribution from biological activity to the CDOM reservoir in the offshore region, although wa-

ter mass mixing was still the dominant factor affecting CDOM distribution.

4.3 *Contributions of different water masses: multi-end-member mixing model*

The absorption coefficient (a_{280}) and salinity were strongly linearly correlated as shown in Table 2, and the main controlling factor of CDOM distribution in the Taiwan Strait was water mass mixing as described in Section 4.2. Such conservative or quasi-conservative feature of CDOM absorption properties in the Taiwan Strait makes it a suitable tracer to evaluate the contributions of different water masses on CDOM inputs in this complex hydrodynamic environment (Aarup et al., 1996). No matter in winter or summer, there are three main endmembers in the Taiwan Strait. Thus, the salinity (S_{al}) and CDOM absorption in the Taiwan Strait can be modeled by a three-end-member mixing model, as expressed by the following equations (Stedmon et al., 2010):

$$S_{\mathrm{al}} = f_{\mathrm{A}} S_{\mathrm{al,A}} + f_{\mathrm{B}} S_{\mathrm{al,B}} + f_{\mathrm{C}} S_{\mathrm{al,C}}, \quad (3)$$

$$a_{280} = f_{\mathrm{A}} a_{280,\mathrm{A}} + f_{\mathrm{B}} a_{280,\mathrm{B}} + f_{\mathrm{C}} a_{280,\mathrm{C}}, \quad (4)$$

$$1 = f_{\mathrm{A}} + f_{\mathrm{B}} + f_{\mathrm{C}}, \quad (5)$$

where f represents the fraction of each water mass; A, B and C represent the SCSW surface flow, the SCSW bottom flow and the continental runoff respectively in summer, or the ZCC, KBC and the continental runoff respectively in winter.

The eigenvalues used to calculate the fraction of each water mass are shown in Table 4. The endmember a_{280} values for the continental runoff were their "apparent abundance" calculated in Table 2 while the salinity values were assumed to be 0.1. The eigenvalues for other water masses were chosen based on their characteristic a_{280} and salinity values. The results show that in summer the fraction of the SCSW surface flow, the SCSW bottom flow and the Continental runoff were 12.4%, 85.0% and 2.5%, respectively. While in winter, the fraction of the ZCC, KBC and the continental runoff were 29.1%, 66.5% and 4.4%. It is noteworthy that whether in summer or winter, the fraction of the continental runoff was small. This is similar to the case in the Baltic Sea (Stedmon et al., 2010). This implies that the influence of direct terrestrial discharge into the coastal Taiwan Strait was limited in normal weather conditions, except for the strong signal disturbance caused by large river plumes during the rainstorm events. These results demonstrate the great potential of using a multi-end-member mixing model in identifying the contribution of freshwater discharge with respect to the CDOM pool in coastal environments.

Table 4. Eigenvalues used for three-end-member model

Season	Endmember	a_{280}/m^{-1}	Salinity
Summer	the continental runoff	7.96	0.100 0
	the SCSW bottom flow	0.92	34.234 6
	the SCSW surface flow	0.94	33.530 0
Winter	the continental runoff	11.71	0.100 0
	ZCC	1.75	31.368 7
	KBC	0.67	34.496 4

5 Conclusions

The Taiwan Strait is a typical channel sea area and is strongly influenced by the East Asian monsoon. Investigations carried out during summer (July to August of 2006) and winter (from December 2006 to January of 2007) seasons demonstrate that the spatial and temporal variability of CDOM in this region was mainly controlled by water mass movement, i.e., Zhemin Coastal Current (ZCC) and the Kuroshio Branch Current (KBC) in winter and the South China Sea Water (SCSW) in summer. These results demonstrate that CDOM optical properties may also be a suitable indicator to trace the hydrologic inputs for other Chinese marginal seas which are also influenced by the Asian monsoon.

Acknowledgements

The authors would like to thank Xu Jing for her help in the calculation of spectral data. Dr. Rob Spencer is thanked for his comments and assistance with English.

References

Aarup T, Holt N, Hojerslev N K. 1996. Optical measurements in the North Sea—Baltic Sea transition zone: II. Water mass classification along the Jutland west coast from salinity and spectral irradiance measurements. Continental Shelf Research, 16(10): 1343–1353

Blough N V, Del Vecchio R. 2002. Chromophoric DOM in the coastal environment. In: Hansell D A, Carlson C A, eds. Biogeochemistry of Marine Dissolved Organic Matter. Amsterdam: Academic Press, 509–546

Bricaud A, Morel A, Prieur L. 1981. Absorption by dissolved organic matter of the sea (yellow substance) in the UV and visible domains. Limnology and Oceanography, 26: 43–53

Doxaran D, Froidefond J M, Lavender S J, et al. 2002. Spectral signature of highly turbid waters: Application with SPOT data to quantify suspended particulate matter concentrations. Remote Sensing of Environment, 81(1): 149–161

Du Cuifen, Shang Shaoling, Dong Qiang, et al. 2010. Characteristics of chromophoric dissolved organic matter in the nearshore waters of the western Taiwan Strait. Estuarine, Coastal and Shelf Science, 88(3): 350–356

Granskog M A, Macdonald R W, Mundy C J, et al. 2007. Distribution, characteristics and potential impacts of chromophoric dissolved organic matter (CDOM) in Hudson Strait and Hudson Bay, Canada. Continental Shelf Research, 27(15): 2032–2050

Guo Weidong, Stedmon C A, Han Yuchao, et al. 2007. The conservative and non-conservative behavior of chromophoric dissolved organic matter in Chinese estuarine waters. Marine Chemistry, 107(3): 357–366

Guo Weidong, Xu Jing, Wang Jiangping, et al. 2010. Characterization of dissolved organic matter in urban sewage using excitation emission matrix fluorescence spectroscopy and parallel factor analysis. Journal of Environmental Sciences, 22: 1728–1734

Guo Weidong, Yang Liyang, Hong Huasheng, et al. 2011a. Assessing the dynamics of chromophoric dissolved organic matter in a subtropical estuary using parallel factor analysis. Marine Chemistry, 124(1–4): 125–133

Guo Weidong, Yang Liyang, Wang Fuli, et al. 2011b. Parallel factor analysis for excitation emission matrix fluorescence spectroscopy of dissolved organic matter from a reservoir-type river. Spectroscopy and Spectral Analysis (in Chinese), 31(2): 427–430

Helms J R, Stubbins A, Ritchie J D, et al. 2008. Absorption spectral slopes and slope ratios as indicators of molecular weight,source and photobleaching of chromophoric dissolved organic matter. Limnol Oceanogr, 53(3): 955–969

Hong Huasheng, Yang Liyang, Guo Weidong, et al. 2012. Characterization of dissolved organic matter under contrasting hydrologic regimes in a subtropical watershed using PARAFAC model. Biogeochemistry, 109: 163–174

Hu Jianyu, Kawamura H, Li Chunyan, et al. 2010. Review on current and seawater volume transport through the Taiwan Strait. Journal of Oceanography, 66(5): 591–610

Jan Sen, Wang Joe, Chem Ching-sheng, et al. 2002. Seasonal variation of the circulation in the Taiwan Strait. Journal of Marine Systems, 35(3–4): 249–268

Jiang Fenghua, Lee F, Wang Xiaoru, et al. 2008. The application of Excitation/Emission Matrix Spectroscopy combined with Multivariate analysis for the characterization and Source identification of Dissolved Organic Matter in Seawater of Bohai Sea, China. Marine Chemistry, 110(1–2): 109–119

Kester D R, Fox M F. 1993. Chemical and biological remote sensing of the South China Sea: satellite and in situ observations. In: Proceeding Environment '93—Symposium on Remote Sensing in Environmental Research and Global Change. Hong Kong: The Commercial Press, 60–72

Kowalczuk P, Durako M J, Young H, et al. 2009. Characterization of dissolved organic matter fluorescence in the South Atlantic Bight with use of PARAFAC model: Interannual variability. Marine Chemistry, 113(3–4): 182–196

Lan Kuowei, Kawamura H, Lee Ming-an, et al. 2009. Summertime sea surface temperature fronts associated with upwelling around the Taiwan Bank. Continental Shelf Research, 29(7): 903–910

Rochelle-Newall E J, Fisher T R. 2002. Production of chromophoric dissolved organic matter fluorescence in marine and estuarine environments: an investigation into the role of phytoplankton. Marine Chemistry, 77(1): 7–21

Stedmon C A, Markager S, Kasa H. 2000. Optical properties and signatures of chromophoric dissolved organic matter (CDOM) in Danish coastal waters. Estuarine, Coastal and Shelf Science, 51(2): 267–278

Stedmon C A, Markager S. 2003. Behaviour of the optical properties of coloured dissolved organic matter under conservative mixing. Estuarine, Coastal and Shelf Science, 57(5–6): 973–979

Stedmon C A, Osburn C L, Kragh T. 2010. Tracing water mass mixing in the Baltic-North Sea transition zone using the optical properties of coloured dissolved organic matter. Estuarine, Coastal and Shelf Science, 87(1): 126–162

Wu Boyu. 1982. Some problems on circulation study in Taiwan Strait. Journal of Oceanography in Taiwan Strait (in Chinese), 1(1): 1–7

Xiao Hui, Cai Shuhui. 1988. Distribution characters of sea temperature and salinity in western Taiwan Strait. Journal of Oceanography in Taiwan Strait (in Chinese), 7: 227–234

Yamashita Y, Maie N, Briceno H, et al. 2010. Optical characterization of dissolved organic matter in tropical rivers of the Guayana Shield, Venezuela. Journal of Geophysics Research, 115: G00F10, doi:10.1029/2009JG000987

Zhang Yunlin, van Dijk M A, Liu Mingliang, et al. 2009. The contribution of phytoplankton degradation to chromophoric dissolved organic matter (CDOM) in eutrophic shallow lakes: Field and experimental evidence. Water Research, 43(18): 4685–4697